Journal of Alloys and Compounds 507 (2010) 215–224

Contents lists available at ScienceDirect

Journal of Alloys and Compounds

journal homepage: www.elsevier.com/locate/jallcom

The study of mechanical properties of Sn–Ag–Cu lead-free solders with different Ag contents and Ni doping under different strain rates and temperatures

F.X. Che[a,b,*], W.H. Zhu[b], Edith S.W. Poh[b], X.W. Zhang[a], X.R. Zhang[b]

[a] Institute of Microelectronics, A*STAR (Agency for Science, Technology and Research), 11 Science Park Road, Singapore Science Park II, Singapore 117685, Singapore
[b] United Test and Assembly Center Ltd., 5 Serangoon North Ave 5, Singapore 554916, Singapore

ARTICLE INFO

Article history:
Received 21 April 2010
Received in revised form 19 July 2010
Accepted 22 July 2010
Available online 3 August 2010

Keywords:
Lead-free solders
Sn–Ag–Cu
Mechanical property
Microstructure
Strain rate

ABSTRACT

In this paper, the tensile tests were conducted at 25 °C to investigate the effect of Ag content and Ni doping on the microstructures and mechanical properties of Sn–3.0Ag–0.5Cu, Sn–2.0Ag–0.5Cu, Sn–1.0Ag–0.5Cu, Sn–1.0Ag–0.5Cu–0.05Ni and Sn–1.0Ag–0.5Cu–0.02Ni solders. The effect of strain rate on mechanical properties was investigated for each solder using stain rates of $10^{-5}\,s^{-1}$, $10^{-4}\,s^{-1}$, $10^{-3}\,s^{-1}$, $10^{-2}\,s^{-1}$ and $10^{-1}\,s^{-1}$. In addition, the effect of temperature on mechanical properties was investigated for Sn–1.0Ag–0.5Cu–0.02Ni solder by conducting tests at −35 °C, 25 °C, 75 °C and 125 °C. Test results show that the elastic modulus, yield stress and ultimate tensile strength increase with increasing strain rate and Ag content, but they decrease with increasing temperature. The elastic modulus, yield stress and ultimate tensile strength are lower and the elongation is larger for Sn–1.0Ag–0.5Cu–0.05Ni solder compared with Sn–1.0Ag–0.5Cu–0.02Ni solder. The strain rate and Ag content dependent mechanical property models have been developed for Sn–Ag–Cu solders for the first time. In addition, the temperature and rate-dependent mechanical property models have also been developed for Sn–1.0Ag–0.5Cu–0.02Ni solder. The microstructures of solders were also analyzed. The Ag content affects Ag_3Sn intermetallic compound dispersion and Sn dendrite size. The microstructures of solder have fine Sn dendrites and more dispersed IMC particles for the high Ag content solder, which makes the solder exhibit high strength and yield stress.

1. Introduction

With the increasing requirement for lead-free solders, it is useful to understand how different solders affect the reliability of microelectronic assembly when subjected to different loading conditions such as thermal cycling, bending, vibration and drop impact. The Sn–Ag–Cu solder is one commonly used lead-free solder in surface mount technology (SMT) assembly for microelectronics. Many studies were conducted on Sn–Ag–Cu lead-free solders [1–30]. Results showed that the Ag content affects thermal fatigue life and drop lifetime for the soldered assembly with Sn–*x*Ag–Cu lead-free solder joint. The thermal fatigue life increases with increasing Ag content in Sn–*x*Ag–Cu lead-free solders due to the Ag content affecting solder fatigue resistance and mechanical properties [2]. However, the drop performance of electronic assembly with Sn–*x*Ag–Cu lead-free solder joint is worsened with increasing Ag content in Sn–*x*Ag–Cu solder [3]. Hence, the different effect trends of Ag content on thermal fatigue life and drop performance were obtained. In order to improve drop performance without reducing the thermal fatigue life of the electronic assembly with Sn–Ag–Cu lead-free solders, some metal additives, such as Ni, Zn, Fe, Co and rare-earth (RE) elements, have been introduced into Sn–Ag–Cu solders to refine the microstructures and reduce the intermetallic compound growth [4–10,13–22]. Among the additives, Ni is one dominant and widely used doping material in Sn–Ag–Cu solders due to its excellent performance in improving solder microstructure, reducing IMC growth and increasing the drop lifetime of electronic assembly [4–10]. Liu et al. [8] reported that the Ni addition has a positive effect on the growth of $(CuNi)_6Sn_5$ layer but negative effect on the growth of Cu_3Sn layer around the interface between Sn–3.8Ag–0.7Cu–*x*Ni solder and Cu substrate during isothermal aging condition and that the IMC grains are refined with the Ni addition increasing. The Cu_3Sn growth is usually linked to the formation of Kirkendall voids, which in turn increases the potential of interfacial brittle fracture [11]. As a result, drop test performance is improved for Sn–Ag–Cu solder joints with a small amount of Ni addition due to thickness reduction of the refined Cu_3Sn layer [12]. The study by Wang et al. [9,10] showed that the minimum effective Ni addition to Sn–2.5Ag–0.8Cu solder is in a range of 0.01–0.03 wt.%. This is effective in suppressing the Cu_3Sn growth and does not cause

* Corresponding author. Present address: Institute of Microelectronics, 11 Science Park Road, Singapore 117685, Singapore. Tel.: +65 67705447; fax: +65 67745747.
E-mail addresses: chefx@ime.a-star.edu.sg, chefaxing@pmail.ntu.edu.sg (F.X. Che).

0925-8388/$ – see front matter © 2010 Elsevier B.V. All rights reserved.
doi:10.1016/j.jallcom.2010.07.160

an excessive Cu_6Sn_5 growth during the reflow stage and aging condition. Recently, some researchers found that the addition of RE elements in Sn–Ag–Cu solders can refine the microstructure and improve the tensile strength and wettability [14–22]. Wang et al. [17] reported that the solderability and mechanical properties of Sn–3.8Ag–0.7Cu solder can be improved by adding light RE Ce in a range of 0.03–0.05 wt.% because the Ce makes the Cu_6Sn_5 and Ag_3Sn precipitates become smaller and uniformly distributed. The creep rupture time of Sn–3.8Ag–0.7Cu solder can be improved by adding 0.05 wt.% Ce as creep damages are reduced and microcrack propagation site is changed due to refinement of IMC particles [18]. Shi et al. [19] reported that adding small amount of heavy RE Er can also improve the wettability, mechanical strength and creep rupture life of Sn–3.8Ag–0.7Cu solder alloy due to the refining of IMC particles and the proper Er content in solder should be in a range of 0.05–0.25 wt.%. Noh et al. [20] investigated the effect of adding Ce to low Ag content solder (Sn–1.0Ag) on microstructure, wettability and mechanical properties using three Ce contents of 0.1 wt.%, 0.2 wt.%, and 0.3 wt.%. The results showed that the microstructures of Sn–1.0Ag–*x*Ce solder become finer and the tensile strength of solder increases with increasing Ce, but the wettability increases in the order: Sn–1.0Ag–0.3Ce, Sn–1.0Ag–0.5Ce and Sn–1.0Ag–0.1Ce [20]. The RE elements are known to be easily oxidized and the excessive RE addition would deteriorate the microstructure and wettability. The rapid growth of tin whiskers has been observed on the surface of Sn–3.0Ag–0.5Cu–0.5Ce solder joints of ball grid array (BGA) packages due to the coarse $CeSn_3$ intermetallic cluster effect [21]. The rapid tin whisker growth can be prevented by adding 0.2 wt.% Zn into Sn–3.0Ag–0.5Cu–0.5Ce solder and the tensile strength of Sn–3.0Ag–0.5Cu–0.5Ce–0.2Zn solder improved significantly compared with that of Sn–3.0Ag–0.5Cu–0.5Ce solder [22]. However, the long-term reliability, such as thermal cycling and the electromigration effect due to high current density, are not clear for lead-free solders with RE addition compared with Ni doped solders, which needs to be investigated. So far, most of the studies focused on the effects of Ag content and metal additions on the solder microstructures [7–10,13–25]. Even though some researchers [2,26,27] investigated the effect of Ag content on fracture behavior and fatigue properties of Sn–Ag–Cu solder, there is a lack of a systematic investigation in the effect of Ag content and metal additions on the mechanical properties of Sn–Ag–Cu solders, e.g., elastic modulus and yield stress. Such mechanical property data are essential for finite element modeling and simulation to help in the design-for-reliability of electronic assembly. Therefore, the main objective of this paper is to develop the Ag content dependent, strain rate-dependent and temperature dependent mechanical property models for Sn–Ag–Cu solders.

In this paper, the effect of Ag content on the mechanical properties of Sn–*x*Ag–0.5Cu solders and the effect of Ni addition on the mechanical properties of Sn–1.0Ag–0.5Cu solder were investigated through the tensile tests for bulk solder specimens. Based on Pang's investigation, the mechanical properties of lead-free solder were similar for both bulk solder and solder joint [28]. So the mechanical properties from bulk solder test can be used in finite element modeling and simulation for the stress–strain behavior evaluation of microscale solder joint. It is known that solder mechanical properties vary significantly with temperature and strain rate [28–30]. In this paper, three different Ag contents including 1 wt.%, 2 wt.% and 3 wt.% Ag in Sn–*x*Ag–0.5Cu solders, and two Ni additives including 0.02 wt.% and 0.05 wt.% Ni in Sn–1.0Ag–0.5Cu solder were investigated. The mechanical properties such as elastic modulus, ultimate tensile strength (UTS), yield stress and elongation, were compared for different solders. The effect of strain rate on the mechanical properties of Sn–Ag–Cu solders was also investigated in a range from $10^{-5}\,s^{-1}$ to $10^{-1}\,s^{-1}$, which covered the solder strain rate encountered in thermal cycling, mechanical cyclic bending and vibration loads. The microstructures of different solders were also analyzed based on scanning electron microscope (SEM) images. In addition, different testing temperature conditions including −35 °C, 25 °C, 75 °C and 125 °C were used for Sn–1.0Ag–0.5Cu–0.02Ni solder to investigate the effect of temperature on the mechanical properties of solder.

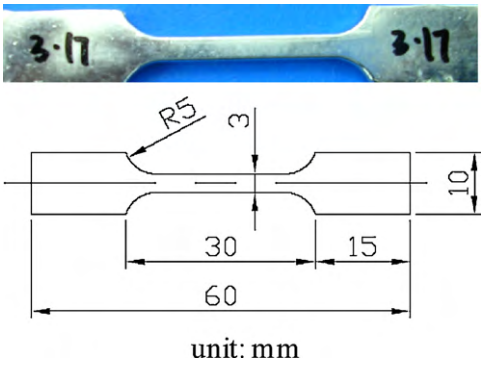

Fig. 1. Geometry of solder specimen.

2. Experimental procedures

The Sn–Ag–Cu bulk solder specimens with flat dog-bone shape were used in this work. Fig. 1 shows the solder bar specimen and its dimensions. The thickness of solder bar is 3 mm. The solder alloys were melted and maintained 100 °C above their respective melting point for 20 min. The bulk solder specimens were cast inside the designed aluminum mold, which was preheated to 120 °C above the melting points of the solder alloys. Then, the specimens were naturally air-cooled at ambient temperature (25 °C). Before the testing, the specimen was annealed at 100 °C for 2 h to reduce the residual stress induced in the sample preparation. Then, the solder bar was fixed onto a testing grip at two ends of specimen using a universal tester as shown in Fig. 2. An extensometer was secured onto the specimen surface to measure the strain of solder. In this work, a length of 10 mm was used as a gauge length. Tensile force added on the specimen was measured by a load cell for stress calculation. The stress–strain curve can be obtained from the measurement data by extensometer and load cell. The strain rate can be controlled by adjusting loading speed. For testing conditions at high and low temperatures, a thermal chamber was used to enclose the tested specimen to provide the designed temperature condition.

This paper focuses on the effect of Ag content, Ni doping, strain rate and temperature on the mechanical material properties of lead-free solders. Five different solders were prepared with the following nominal composition: Sn–3.0Ag–0.5Cu (SAC305), Sn–2.0Ag–0.5Cu (SAC205), Sn–1.0Ag–0.5Cu (SAC105), Sn–1.0Ag–0.5Cu–0.05Ni (SAC105Ni0.05) and Sn–1.0Ag–0.5Cu–0.02Ni (SAC105Ni0.02). Table 1 lists the detailed chemical compositions of five solder alloys. Five samples were tested under the same testing condition for each solder specimen to obtain the reliable and repeatable results. Then, the mechanical properties were obtained by averaging testing data. The tensile tests were conducted at room temperature (25 °C) for SAC305, SAC205, SAC105, SAC105Ni0.05 and SAC105Ni0.02 solders under different strain rates of $10^{-5}\,s^{-1}$, $10^{-4}\,s^{-1}$, $10^{-3}\,s^{-1}$, $10^{-2}\,s^{-1}$, and $10^{-1}\,s^{-1}$, respectively to investigate the effect of Ag content, Ni additive and strain rate on the mechanical properties of solder, such as elastic modulus, yield stress, ultimate tensile strength (UTS) and elongation. In this paper, the elastic modulus, also called Young's modulus, of solder was obtained from the elastic part of the tensile stress–strain curve. The yield stress of solder was considered as the stress value at which 0.2% plastic strain occurs. The UTS of solder was considered as the maximum stress in the stress–strain curve. In addition, the effect of temperature on the mechanical properties of SAC105Ni0.02 solder was investigated by conducting tests at at −35 °C, 25 °C, 75 °C and 125 °C, so as to develop the temperature dependent mechanical properties for SAC105Ni0.02 solder.

The microstructures of solders were analyzed based on the scanning electron microscope (SEM) images. The SEM samples were prepared by dicing, resin molding, grinding and polishing processes. The effects of Ag content on IMC distribution and Sn dendrite were examined to understand the effect of Ag content on the mechanical properties of solders.

3. Results and discussion

3.1. Effect of strain rate on solder mechanical properties

Fig. 3 shows the typical ductile failure mode of Sn–3.0Ag–0.5Cu solder. Necking and surface coarsening phenomena were observed

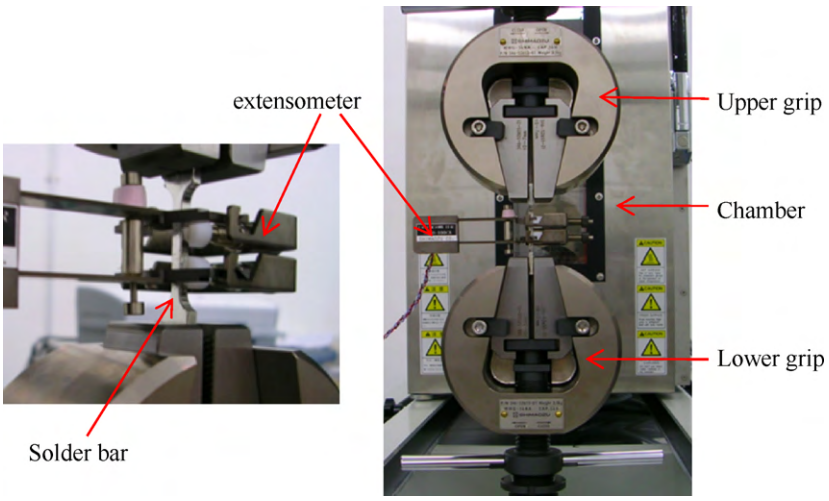

Fig. 2. Tensile testing setup.

Table 1
Chemical compositions for solders used in this study (wt.%).

Alloy	Sn	Ag	Cu	Ni
SAC105	Balance	1.01	0.518	<0.001
SAC205	Balance	1.99	0.521	<0.001
SAC305	Balance	2.98	0.527	<0.001
SAC105Ni0.02	Balance	1.01	0.518	0.0197
SAC105Ni0.05	Balance	1.01	0.518	0.0498

Fig. 3. Typical ductile failure mode of Sn–3.0Ag–0.5Cu solder.

for the tested solder before complete failure. The stress–strain curves of Sn–1.0Ag–0.5Cu–0.02Ni solder are shown in Fig. 4. It shows that strain rate affects mechanical properties significantly. The solder exhibits significant ductility with large elongation and plastic deformation before fracture. The yield stress, UTS and elongation increase with increasing strain rate. Fig. 5 shows the mechanical properties of elastic modulus, yield stress, UTS, elongation at UTS (UE) and total elongation for different Sn–Ag–Cu solders with varying tensile strain rates. Different solders show the similar trend with strain rate effect. The elastic modulus, E, of solder is determined by the initial slope of the elastic part of stress–strain curve. The yield stress, σ_y, of solder is considered as the stress value at which 0.2% plastic strain occurs. After yield, the solder shows more ductility due to creep effect. The UTS of solder is considered as the maximum stress in the stress–strain curve. The elongation corresponding to the UTS and the total elongation at the solder specimen fracture point increase with increasing strain rate. When the tensile test is conducted under a low strain rate, the solder creep effect is significant, so the elastic modulus, yield stress and UTS decrease due to creep behavior. When the solder is tested under a large strain rate, the testing time to solder fracture failure is so short that the creep of solder cannot be fully developed. Therefore, the solder exhibits higher elastic modulus, yield stress and UTS.

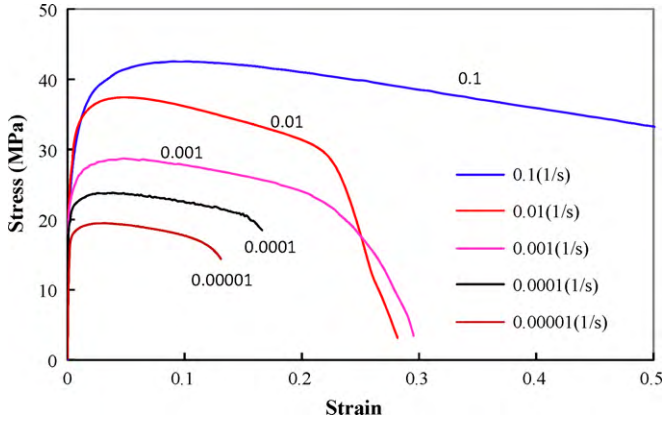

Fig. 4. Effect of strain rate on the stress–strain curve of Sn–1.0Ag–0.5Cu–0.02Ni solder.

From the testing result analysis, the relationship between mechanical properties and strain rate can be determined through curve-fitting. Figs. 6–8 show the relationship between strain rate and elastic modulus, yield stress and UTS for different solders. The elastic modulus, yield stress and UTS increase with increasing strain rate for all solders. The solder with high Ag content exhibits larger elastic modulus, yield stress and UTS compared with the solder with low Ag content. The effect of Ni additive on mechanical properties under different strain rates is much more complicated than the effect of Ag content on mechanical properties. The effect of Ag content and Ni additive on mechanical properties will be discussed in the subsequent sections. The logarithmic relationship between elastic modulus and strain rate can be obtained from Fig. 6. The power relationship between yield stress, UTS and strain rate can be found from Figs. 7 and 8.

The strain rate-dependent material property models of Sn–Ag–Cu solders including the elastic modulus of E, yield stress of σ_y and UTS can be written as follows:

$$E(\dot{\varepsilon})_{\text{Sn–Ag–Cu}} = a_1 \log(\dot{\varepsilon}) + a_2 \quad (1)$$

$$\sigma_y(\dot{\varepsilon})_{\text{Sn–Ag–Cu}} = b_1(\dot{\varepsilon})^{b_2} \quad (2)$$

$$\text{UTS}(\dot{\varepsilon})_{\text{Sn–Ag–Cu}} = c_1(\dot{\varepsilon})^{c_2} \quad (3)$$

where a_1, a_2, b_1, b_2, c_1, and c_2 are material constants, which are obtained from curve-fitting and listed in Table 2 for different solders. The calculated values and errors of the mechanical properties compared with the test results are listed in Table 3. It can be seen that the curve-fitting models are accurate with the errors within 13.1% for the predicted elastic modulus, 6.6% for the predicted yield stress and 5.0% for the predicted UTS. The above rate-dependent

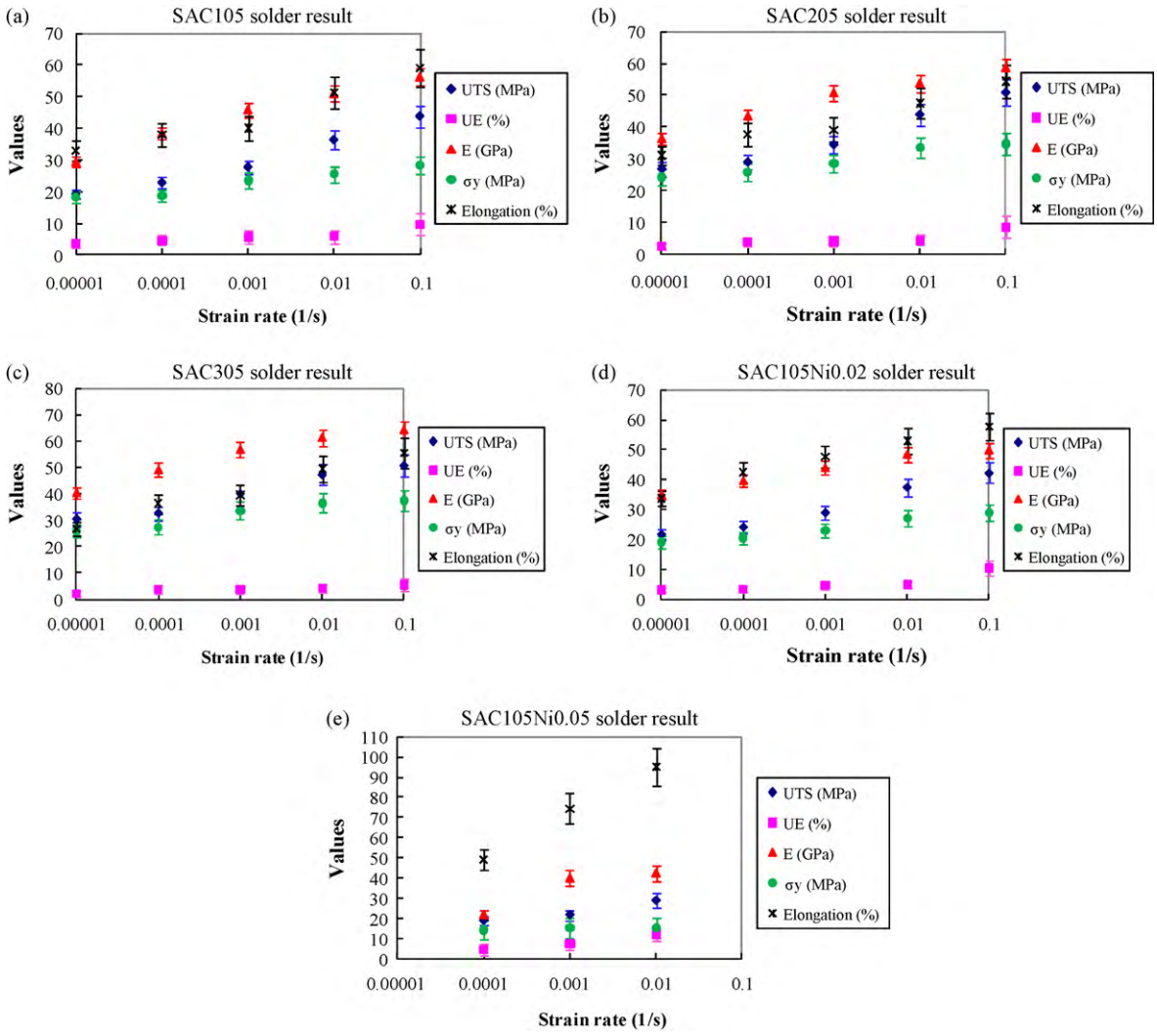

Fig. 5. Effect of strain rate on the mechanical properties of Sn–Ag–Cu solders: a) SAC105, b) SAC205, c) SAC305, d) SAC105Ni0.02, and e) SAC105Ni0.05.

mechanical models can be implemented in finite element simulation for calculating the material properties of solder to simulate stress behavior when the soldered electronic assemblies are subjected to external loading with various strain rates.

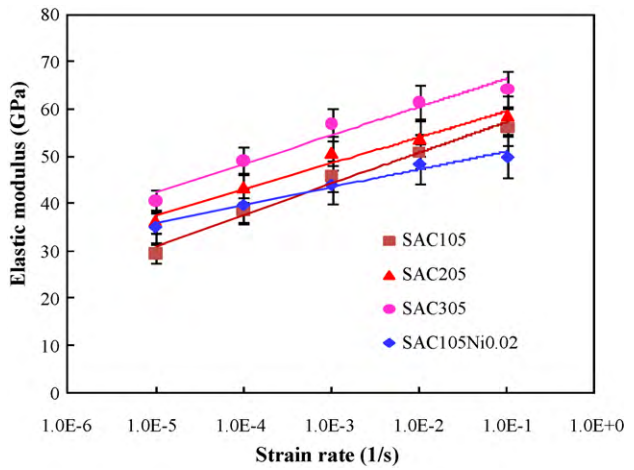

Fig. 6. Relationship between elastic modulus and strain rate for different Sn–Ag–Cu solders.

3.2. Effect of Ag content on solder mechanical properties and microstructures

Fig. 9 shows the stress–strain curves for different Sn–Ag–Cu solders under the same strain rate. The tensile strength of solder increases with increasing the Ag content. Increasing the Ag content in Sn–Ag–Cu solder reduces the ductility. Therefore, the electronic assembly with high Ag content solder joint has lower drop lifetime when subjected to drop impact, which is consistent with the testing results given by Amagai et al. [3]. The low Ag content solders are increasingly used in electronic assembly for handheld electronic products to improve the drop performance of solder joint [3,12].

Figs. 10–12 show the effect of Ag content on the elastic modulus, yield stress and UTS under different strain rates, respectively. It can be seen that the elastic modulus, yield stress and UTS increase with increasing the Ag content for all strain rates. Table 4 lists the Ag content dependent mechanical property models and material constants for Sn–*x*Ag–0.5Cu solders under different strain rates based on a linear regression model. The *x* in Table 4 represents the Ag content in weight percentage value, for example, *x* equals to 1 for Sn–1.0Ag–0.5Cu solder. For a given strain rate, the elastic modulus, yield stress and UTS for Sn–*x*Ag–0.5Cu solder can be calculated by substituting Ag content, *x* into the models in Table 4. From the literature review, this is the first time the Ag content depen-

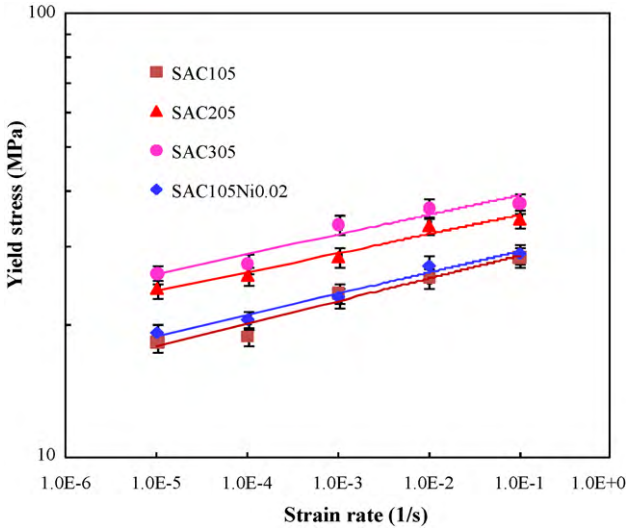

Fig. 7. Relationship between yield stress and strain rate for different Sn–Ag–Cu solders.

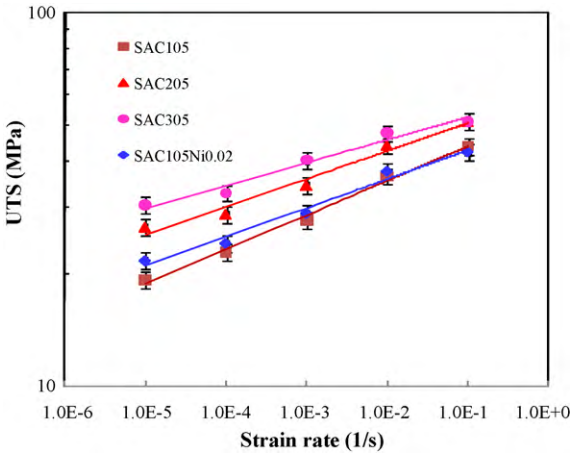

Fig. 8. Relationship between UTS and strain rate for different Sn–Ag–Cu solders.

dent mechanical property models for Sn–Ag–Cu solder have been developed. Such models can be used to calculate the mechanical properties of Sn–Ag–Cu solder when the actual test data are not available.

Table 2
Material constants in the rate-dependent mechanical property models of (1)–(3).

Solders	a_1	a_2 (GPa)	b_1 (MPa)	b_2	c_1 (MPa)	c_2
SAC105	6.56	63.87	32.15	0.0513	53.99	0.0918
SAC205	5.55	65.08	38.96	0.0430	59.90	0.0746
SAC305	5.99	72.43	43.32	0.0445	60.18	0.0608
SAC105Ni200 ppm	3.82	54.86	32.69	0.0483	51.02	0.0775
SAC105Ni500 ppm	10.25	65.29	16.71	0.0173	43.88	0.0960

Table 3
Predicted mechanical property data and errors for different solders at various strain rates.

Solder/strain rate	Calculated values			Errors		
	E (GPa)	Yield (MPa)	UTS (MPa)	E	Yield	UTS
SAC105						
10^{-5} s^{-1}	31.06	17.81	18.76	5.3%	−2.6%	−2.2%
10^{-4} s^{-1}	37.62	20.04	23.18	−2.2%	6.6%	1.8%
10^{-3} s^{-1}	44.18	22.56	28.64	−3.6%	−4.3%	3.4%
10^{-2} s^{-1}	50.75	25.39	35.38	−0.3%	−0.3%	−2.6%
10^{-1} s^{-1}	57.31	28.57	43.70	2.1%	0.8%	−0.1%
SAC205						
10^{-5} s^{-1}	37.33	23.75	25.38	3.4%	−1.2%	−4.6%
10^{-4} s^{-1}	42.88	26.22	30.13	−0.9%	1.9%	4.7%
10^{-3} s^{-1}	48.43	28.95	35.78	−4.4%	2.1%	4.2%
10^{-2} s^{-1}	53.98	31.96	42.48	0.6%	−4.4%	−3.2%
10^{-1} s^{-1}	59.53	35.29	50.45	1.6%	2.0%	−0.8%
SAC305						
10^{-5} s^{-1}	42.50	25.95	29.88	5.0%	0.0%	−1.9%
10^{-4} s^{-1}	48.48	28.75	34.38	−1.4%	4.8%	5.0%
10^{-3} s^{-1}	54.47	31.86	39.54	−4.2%	−5.3%	−1.6%
10^{-2} s^{-1}	60.46	35.29	45.48	−1.6%	−3.3%	−4.0%
10^{-1} s^{-1}	66.44	39.10	52.32	3.3%	4.2%	2.7%
SAC105Ni200 ppm						
10^{-5} s^{-1}	35.75	18.75	20.90	2.1%	−1.8%	−3.3%
10^{-4} s^{-1}	39.57	20.95	24.99	−0.3%	2.4%	3.9%
10^{-3} s^{-1}	43.39	23.42	29.87	−1.3%	1.7%	3.3%
10^{-2} s^{-1}	47.22	26.17	35.71	−2.4%	−3.5%	−4.7%
10^{-1} s^{-1}	51.04	29.25	42.68	2.5%	1.2%	1.0%
SAC105Ni500 ppm						
10^{-4} s^{-1}	24.30	14.25	18.12	11.7%	1.2%	−2.3%
10^{-3} s^{-1}	34.55	14.83	22.61	−13.1%	−2.3%	4.9%
10^{-2} s^{-1}	44.80	15.43	28.20	6.1%	1.2%	−2.4%

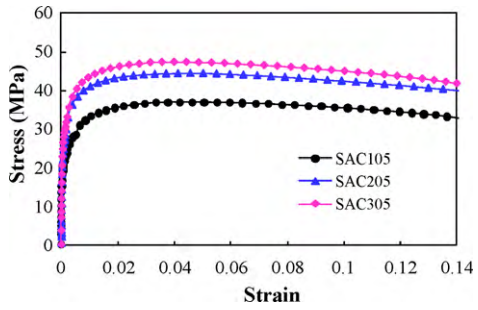

Fig. 9. Effect of Ag content on the stress–strain curves of Sn–Ag–Cu solders.

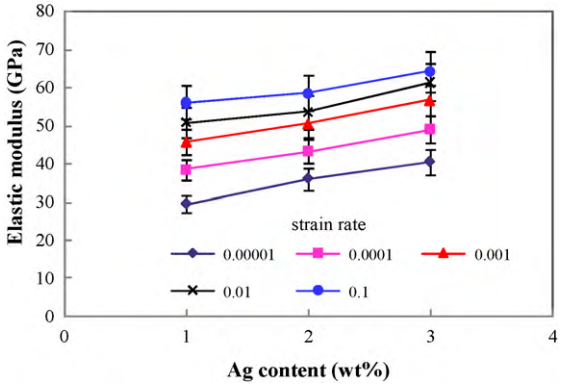

Fig. 10. Effect of Ag content on elastic modulus of Sn–Ag–Cu solder under different strain rates.

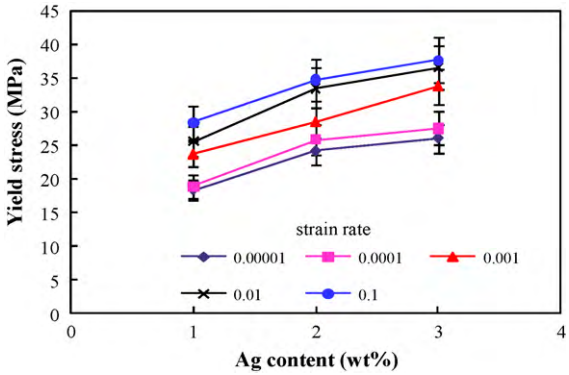

Fig. 11. Effect of Ag content on yield stress of Sn–Ag–Cu solder under different strain rates.

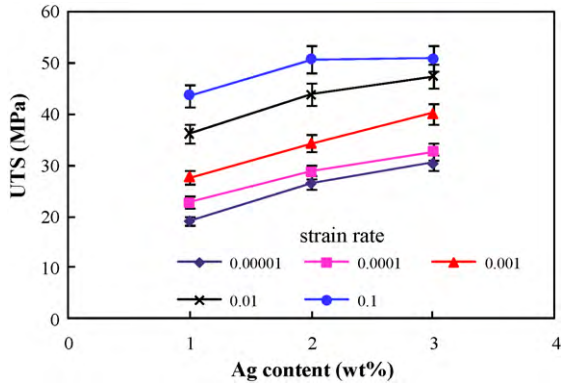

Fig. 12. Effect of Ag content on UTS of Sn–Ag–Cu solder under different strain rates.

In order to further investigate the effect of Ag content on the solder mechanical properties and microstructures, scanning electron microscopy was used to study the microstructures of solders. Fig. 13 shows the SEM images of microstructure for different Sn–Ag–Cu solders. It can be seen that the Ag content affects the Ag_3Sn and Cu_6Sn_5 intermetallic compound (IMC) precipitate. Increasing Ag content in Sn–Ag–Cu solder increases the amount of Ag_3Sn and Cu_6Sn_5 IMCs distributed in a Sn-rich matrix. Therefore, the microstructure of solder has finer Sn dendrites and more IMC precipitates in solder with higher Ag content such as SAC305. This makes the solder exhibit high strength and fatigue resistance because of precipitate strengthening [24]. Thermal fatigue tests done by Terashima et al. [2] showed that the electronic assemblies with high Ag content solder joint exhibited a higher thermal fatigue life. In the meantime, more evenly distributed Ag_3Sn IMC precipitates in the high Ag content solder can suppress the plastic deformation of solder. In the Hall–Petch relation, the yield stress of a given metal material is proportional to $d^{-1/2}$, where d is its average grain size [31]. Merchant et al. [32] has reported that the fine grain size Cu foils have relatively large elastic modulus and yield stress at room temperature.

The low Ag content solders with low elastic modulus and yield stress exhibit relatively high ductility. Figs. 14 and 15 show the total elongation at the solder fracture point and elongation at UTS for different solders. It can be seen that the SAC105 solder has a larger total elongation and UE than the solders of SAC205 and SAC305 due to sparsely distributed Ag_3Sn IMC particles in SAC105 solder. The larger UE and total elongation can improve the solder drop performance because the softer solder joints absorb more dynamic energy and reduce the dynamic stress transferred from printed circuit board (PCB) to IMC/solder interface layer [3,12].

3.3. Development of Ag content and rate-dependent mechanical property models

The two sections above discussed the effects of strain rate and Ag content on mechanical properties separately. For the given solders of SAC105, SAC205 or SAC305, the elastic modulus, yield stress and UTS can be determined by using Eqs. (1)–(3) and Table 2 when the strain rate is known. For a certain strain rate, the mechanical properties can be determined for Sn–xAg–0.5Cu solders by using the models in Table 4. For example, for the Sn–1.2Ag–0.5Cu solder, the mechanical properties can be calculated by substituting $x = 1.2$ into the corresponding model in Table 4. In this section, the effects of Ag content and strain rate on mechanical proper-

Table 4
Mechanical property models and constants for Sn–xAg–0.5Cu solders (x is the Ag content in wt.%).

Strain rate (s^{-1})	$E = aX + b$ (GPa)		$\sigma_y = cX + d$ (MPa)		UTS $= eX + f$ (MPa)	
	a	b (GPa)	c	d (MPa)	e	f (MPa)
0.00001	5.49	24.37	3.84	15.08	5.63	14.15
0.0001	5.34	32.96	4.32	15.36	4.99	18.12
0.001	5.50	40.12	5.04	18.45	6.25	21.57
0.01	5.26	44.81	5.53	20.75	5.55	31.44
0.1	4.10	51.48	4.60	24.30	3.60	41.32

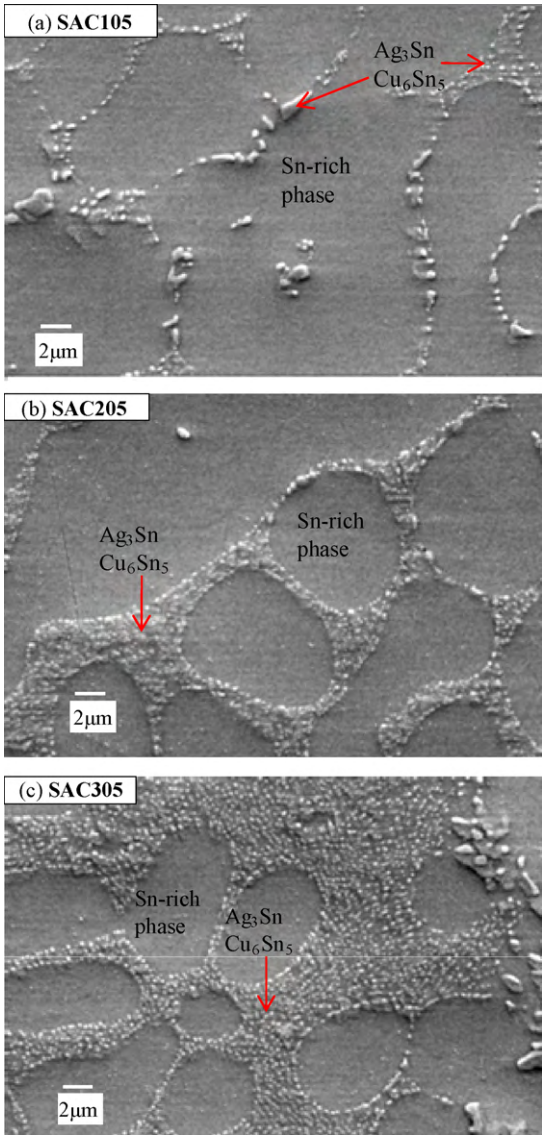

Fig. 13. SEM images of the microstructure of Sn–Ag–Cu solders: a) SAC105, b) SAC205, and c) SAC305.

ties are considered concurrently to develop the uniform Ag content and rate-dependent mechanical property models. Through curve-fitting analysis, the elastic modulus of E, yield stress of σ_y and UTS of solders satisfy the following models:

$$E(X,\dot{\varepsilon})_{\mathrm{Sn}-x\mathrm{Ag}-0.5\mathrm{Cu}} = (a_1X + a_2)\log(\dot{\varepsilon}) + (a_3X + a_4) \quad (4)$$

$$\sigma_y(X,\dot{\varepsilon})_{\mathrm{Sn}-x\mathrm{Ag}-0.5\mathrm{Cu}} = (b_1X + b_2)(\dot{\varepsilon})^{(b_3X+b_4)} \quad (5)$$

$$\mathrm{UTS}(X,\dot{\varepsilon})_{\mathrm{Sn}-x\mathrm{Ag}-0.5\mathrm{Cu}} = (c_1X + c_2)(\dot{\varepsilon})^{(c_3X+c_4)} \quad (6)$$

where x is the Ag content (wt.%) in Sn–xAg–0.5Cu solder. The material constants of a_1, a_2, a_3, and a_4 in the elastic modulus model; b_1, b_2, b_3, and b_4 in the yield stress model; c_1, c_2, c_3, and c_4 in the UTS model are given in Table 5. From the error analysis between the calculated values and the test results, it is found that the curve-fitting Eqs. (4)–(6) are accurate with the errors within 6.0% for the

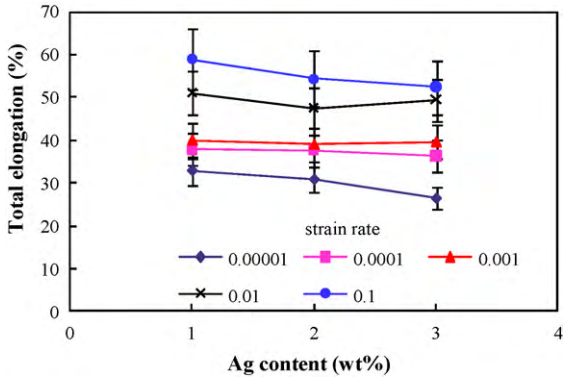

Fig. 14. Effect of Ag content on total elongation of Sn–Ag–Cu solder under different strain rates.

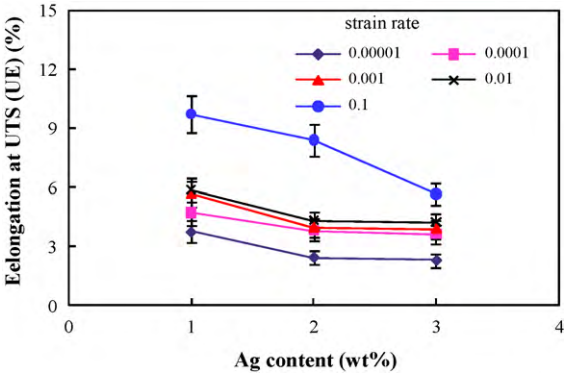

Fig. 15. Effect of Ag content on elongation at UTS of Sn–Ag–Cu solder under different strain rates.

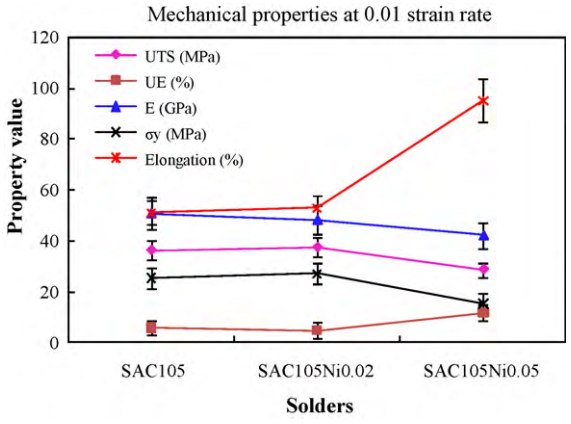

Fig. 16. Effect of Ni additive on the mechanical properties of solder.

Table 5
Material constants in Ag content and rate-dependent mechanical property models of (4)–(6).

Elastic modulus model		Yield stress model		UTS model	
Variable	Value	Variable	Value	Variable	Value
a_1	−0.285	b_1	5.851	c_1	2.870
a_2	6.604	b_2	26.213	c_2	52.596
a_3	4.282	b_3	−0.00166	c_3	−0.0155
a_4	58.559	b_4	0.0483	c_4	0.107

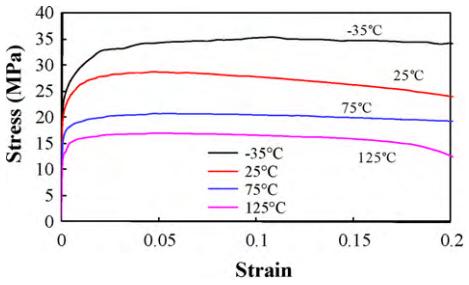

Fig. 17. Effect of temperature on the stress–strain curve of SAC105Ni0.02 solder.

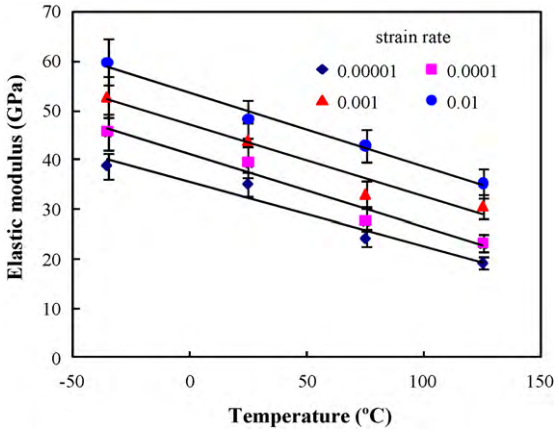

Fig. 18. Effect of temperature on elastic modulus of SAC105Ni0.02 solder.

predicted elastic modulus, 9.0% for the predicted yield stress and 11.0% for the predicted UTS.

3.4. Effect of Ni additive on solder mechanical properties

Two Ni doped solders of SAC105Ni0.02 and SAC105Ni0.05 were chosen for investigating the effect of Ni additive on the mechanical properties of solder. Adding Ni particles in the Sn–Ag–Cu solder improves solder joint drop reliability because Ni additive suppresses the Cu_3Sn IMC growth and improves solder microstructures and tensile properties [4,5,7–10]. More and more lead-free solders with Ni additive are being applied in handheld electronic products. Thus it is necessary to assess the mechanical properties for such solders. Fig. 16 shows the effect of Ni additive on the material properties of solder. It can be seen that 500 ppm Ni additive in solder affects the mechanical properties of solder more significantly com-

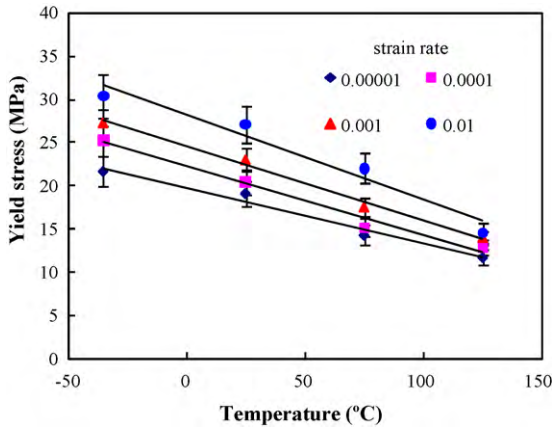

Fig. 19. Effect of temperature on yield stress of SAC105Ni0.02 solder.

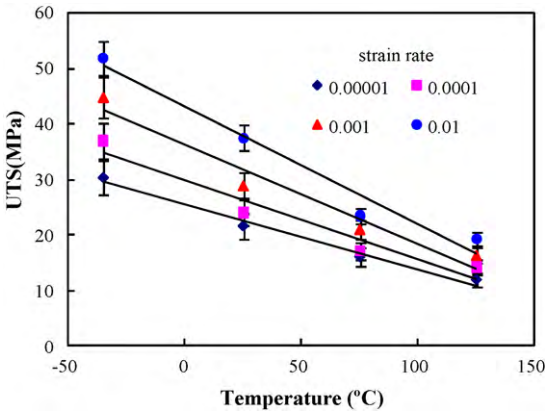

Fig. 20. Effect of temperature on UTS of SAC105Ni0.02 solder.

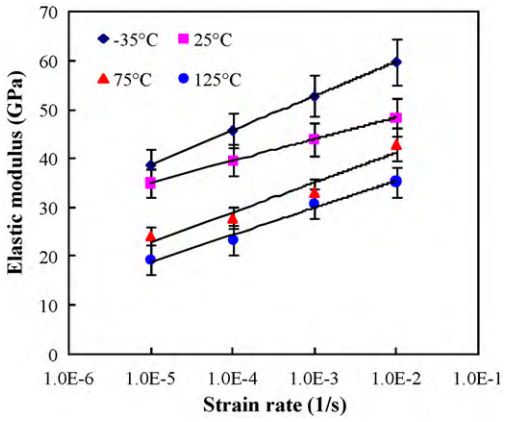

Fig. 21. Effect of strain rate on elastic modulus of SAC105Ni0.02 solder.

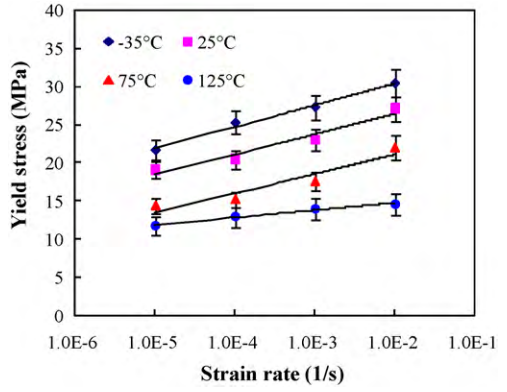

Fig. 22. Effect of strain rate on yield stress of SAC105Ni0.02 solder.

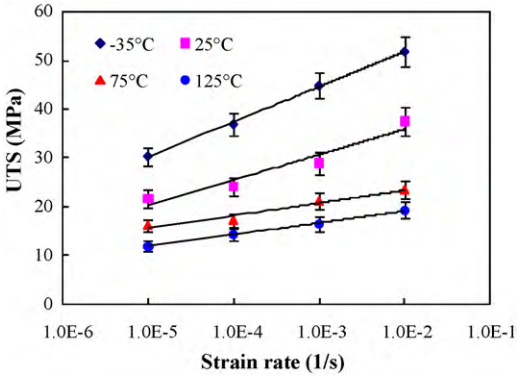

Fig. 23. Effect of strain rate on UTS of SAC105Ni0.02 solder.

Table 6
Material constants in temperature and rate-dependent mechanical property models of (7)–(9).

Elastic modulus model		Yield stress model		UTS model	
Variable	Value	Variable	Value	Variable	Value
a_1	−0.00592	b_1	−0.132	c_1	−0.243
a_2	6.07	b_2	35.57	c_2	59.76
a_3	−0.164	b_3	−4.80E−05	c_3	2.02E−04
a_4	65.59	b_4	0.0513	c_4	0.0745

pared with 200 ppm Ni additive. The SAC105 solder with 500 ppm Ni additive has a lower elastic modulus, UTS and yield stress, but a larger elongation compared with SAC105 solder without Ni doping and SAC105 solder with 200 ppm Ni additive. One possible reason for such phenomena is that with increasing Ni additive, the volume fraction of Sn dendrites decreases and the IMC becomes coarser [33]. This makes SAC105 solder with 500 ppm Ni additive exhibit lower elastic modulus and yield stress. In addition, the peak in fluidity was observed for 500 ppm Ni in Sn-based lead-free solder due to the suppression of Sn dendrites [33], which makes solder with 500 ppm Ni additive exhibit more ductility and larger elongation accordingly. The SAC105 solder with 200 ppm Ni additive shows the similar mechanical properties as SAC105 solder without Ni additive. At a low strain rate regime, the elastic modulus and yield stress of SAC105Ni0.02 solder are slightly higher than those of SAC105 solder (see Figs. 6 and 7). However, at a high strain rate regime, for example, more than 0.01 s^{-1}, the elastic modulus and yield stress of SAC105Ni0.02 solder are lower than those of SAC105 solder. The 200 ppm Ni additive in SAC105 solder reduces the sensitivity of the mechanical property to strain rate. Research revealed that the Ni additive in Sn–Ag–Cu solder increased the impact strength of solder joint based on Izod impact test results [6], which contributed to the improvement of the drop reliability of electronic assembly using Ni doped Sn–Ag–Cu solder joint.

3.5. Development of temperature and rate-dependent mechanical property models for SAC105Ni0.02 solder

In this paper, the correlation between Ni additive and mechanical properties has not been developed systematically compared with the effect Ag content on mechanical properties of solder. However, the tensile tests were conducted comprehensively for SAC105Ni0.02 solder under different temperature conditions and strain rates to develop the temperature and rate-dependent mechanical property models. This solder is widely used and there is currently insufficient data available for finite element modeling and simulation. The temperature ranges from −35 °C to 125 °C and the strain rate varies from 10^{-5} s^{-1} to 10^{-2} s^{-1}, so the developed material models can be used in finite element and simulation for solder joint reliability evaluation when electronic assemblies subject to typical thermal cycling, bending and vibration loads. Fig. 17 shows the typical stress–strain curve of solder under different testing temperatures. It is clear that the solder becomes more ductile and softer when testing temperature increases. Figs. 18–20 show the effect of temperature on the elastic modulus, yield stress and UTS at various strain rates. It can be seen that the elastic modulus, yield stress and UTS decrease with increasing temperature. The effect of temperature on the mechanical properties of solder at a large strain rate is more prominent compared with such effect at a low strain rate. Figs. 21–23 show the effect of strain rate on the elastic modulus, yield stress and UTS at different test temperatures. It can be seen that the elastic modulus, yield stress and UTS increase with increasing strain rate. Large strain rate makes the solder become harder, while high temperature makes the solder become softer.

Based on correlation between the mechanical properties and strain rate or temperature from Figs. 18–23, the rate and temperature dependent mechanical property models have been developed for SAC105Ni0.02 solder:

$$E(T,\dot{\varepsilon})_{\mathrm{SAC105Ni0.02}} = (a_1T + a_2)\log(\dot{\varepsilon}) + (a_3T + a_4) \quad (7)$$

$$\sigma_y(T,\dot{\varepsilon})_{\mathrm{SAC105Ni0.02}} = (b_1T + b_2)(\dot{\varepsilon})^{(b_3T+b_4)} \quad (8)$$

$$\mathrm{UTS}(T,\dot{\varepsilon})_{\mathrm{SAC105Ni0.02}} = (c_1T + c_2)(\dot{\varepsilon})^{(c_3T+c_4)} \quad (9)$$

Table 7
Predicted mechanical property data and errors based on the models of (7)–(9).

Strain rate/temp.	Calculated values			Errors		
	E (GPa)	Yield (MPa)	UTS (MPa)	E	Yield	UTS
10^{-5} s^{-1}						
−35 °C	39.97	22.62	31.42	3.4%	4.5%	3.4%
25 °C	31.89	18.09	21.49	−8.9%	−5.2%	−0.5%
75 °C	25.15	14.34	14.80	3.9%	0.3%	−7.7%
125 °C	18.42	10.62	9.33	−4.5%	−9.3%	−14.4%
10^{-4} s^{-1}						
−35 °C	46.24	25.45	36.70	1.0%	0.8%	−0.7%
25 °C	37.81	20.36	25.81	−4.7%	−0.5%	7.3%
75 °C	30.77	16.14	18.20	10.5%	6.6%	6.2%
125 °C	23.74	11.95	11.73	2.1%	−7.4%	−13.3%
10^{-3} s^{-1}						
−35 °C	52.52	28.60	42.86	−0.5%	4.7%	−4.4%
25 °C	43.73	22.88	31.00	−0.5%	−0.6%	7.1%
75 °C	36.40	18.15	22.37	10.0%	3.5%	6.1%
125 °C	29.07	13.44	14.76	−5.3%	−3.9%	−9.9%
10^{-2} s^{-1}						
−35 °C	58.79	32.09	50.05	−1.7%	5.5%	−3.4%
25 °C	49.64	25.69	37.23	2.6%	−5.2%	−0.7%
75 °C	42.02	20.38	27.50	−1.9%	−7.4%	14.2%
125 °C	34.40	15.10	18.57	−2.5%	3.7%	−3.4%

where T is temperature in °C, $\dot{\varepsilon}$ is strain rate in s^{-1}. The material constants of a_1, a_2, a_3, and a_4 in the elastic modulus model; b_1, b_2, b_3, and b_4 in the yield stress model; c_1, c_2, c_3, and c_4 in the UTS model are listed in Table 6. The error analysis was conducted to evaluate the accuracy of models. The calculated values and errors of the mechanical properties are listed in Table 7. It can be seen that the curve-fitting models are accurate with the errors within 10.5% for the predicted elastic modulus, 9.3% for the predicted yield stress and 14.4% for the predicted UTS. Such models can be used in finite element modeling and simulation for solder joint reliability assessment when the electronic assemblies with SAC105Ni200 solder subject to thermal cycling, mechanical bending or vibration loading.

4. Conclusions

Tensile tests for Sn–1Ag–0.5Cu, Sn–2Ag–0.5Cu, Sn–3Ag–0.5Cu, Sn–1.0Ag–0.5Cu–0.02Ni and Sn–1.0Ag–0.5Cu–0.05Ni solders were conducted. The effects of Ag content, Ni additive, strain rate and temperature on the mechanical properties of solders were investigated. The effect of Ag content on the microstructures of solder was also studied. Some important results and conclusions are summarized as follows:

(1) The elastic modulus, yield stress and UTS of Sn–Ag–Cu solders are highly strain rate and temperature dependent. The elastic modulus, yield stress and UTS increase with increasing strain rate, but decrease with increasing temperature.
(2) The elastic modulus, yield stress and UTS increase with increasing the Ag content. The Ag content dependent mechanical property models are provided for Sn–*x*Ag–0.5Cu solders under different strain rates for the first time.
(3) The strain rate and Ag content dependent mechanical property models for the elastic modulus, yield stress and UTS with satisfactory accuracy have been developed for Sn–Ag–Cu solders for the first time, which can be used to determine the mechanical properties at various loading rates for Sn–Ag–Cu solders with different Ag contents.
(4) The strain rate and temperature dependent mechanical property models for the elastic modulus, yield stress and UTS have been developed for SAC105Ni0.02 solder. Such models can be used in finite element modeling and simulation for solder material to evaluate the thermomechanical or mechanical performance of electronic assemblies.
(5) The microstructure of high Ag content solder has more IMC precipitates and finer Sn dendrites, which makes the solder exhibit high strength.
(6) The elongation at UTS point and total elongation at fracture point increase with increasing strain rate, but decrease with increasing the Ag content.
(7) The Sn–Ag–Cu solder with 500 ppm Ni additive exhibits more ductility (such as larger elongation, lower elastic modulus and yield stress) than Sn–Ag–Cu solder with 200 ppm Ni additive because of the peak in fluidity, the suppression of Sn dendrites and IMC growth observed in solder with 500 ppm Ni additive [33].

References

[1] M. Amagai, M. Watanabe, M. Omiya, K. Kishimoto, T. Shibuya, Microelectron. Reliab. 42 (2002) 951–966.
[2] S. Terashima, Y. Kariya, T. Hosoi, M. Tanaka, J. Electron. Mater. 32 (2003) 1527–1533.
[3] M. Amagai, Y. Toyoda, T. Tajima, Proceedings of Electronic Components and Technology Conference, 2003, pp. 317–322.
[4] K.S. Kim, S.H. Huh, K. Suganuma, Microelectron. Reliab. 43 (2003) 259–267.
[5] M. Amagai, Proceedings of Electronic Components and Technology Conference, 2006, pp. 1170–1190.
[6] I.E. Anderson, J. Mater. Sci.: Mater. Electron. 18 (2007) 55–76.
[7] T. Laurila, J. Hurtig, V. Vuorinen, J.K. Kivilahti, Microelectron. Reliab. 49 (2009) 242–247.
[8] P. Liu, P. Yao, J. Liu, J. Alloys Compd. 486 (2009) 474–479.
[9] Y.W. Wang, Y.W. Lin, C.T. Tu, C.R. Kao, J. Alloys Compd. 478 (2009) 121–127.
[10] Y.W. Wang, C.C. Chang, C.R. Kao, J. Alloys Compd. 478 (2009) L1–L4.
[11] L.H. Xu, J.H.L. Pang, F.X. Che, J. Electron. Mater. 37 (2008) 880–886.
[12] W.H. Zhu, L.H. Xu, J.H.L. Pang, X.R. Zhang, E. Poh, Y.F. Sun, A.Y.S. Sun, C.K. Wang, H.B. Tan, Proceedings of Electronic Components and Technology Conference, 2008, pp. 1667–1672.
[13] S.K. Kang, D. Leonard, D.Y. Shih, L. Gignac, D.W. Henderson, S. Cho, J. Yu, J. Electron. Mater. 35 (2006) 479–485.
[14] C.M.L. Wu, Y.W. Wong, J. Mater. Sci.: Mater. Electron. 18 (2007) 77–91.
[15] C.M.T. Law, C.M.L. Wu, D.Q. Yu, L. Wang, J.K.L. Lai, J. Electron. Mater. 35 (2006) 89–93.
[16] B. Li, Y. Shi, Y. Lei, F. Guo, Z. Xia, B. Zong, J. Electron. Mater. 34 (2005) 217–224.
[17] J.X. Wang, S.B. Xue, Z.J. Han, S.L. Yu, Y. Chen, Y.P. Shi, H. Wang, J. Alloys Compd. 467 (2009) 219–226.
[18] W. Xiao, Y. Shi, G. Xu, R. Ren, F. Guo, Z. Xia, Y. Lei, J. Alloys Compd. 472 (2009) 198–202.
[19] Y. Shi, J. Tian, H. Hao, Z. Xia, Y. Lei, F. Guo, J. Alloys Compd. 453 (2008) 180–184.
[20] B.I. Noh, J.H. Choi, J.W. Yoon, S.B. Jung, J. Alloys Compd. 499 (2010) 154–159.
[21] T.H. Chung, S.F. Yen, J. Eletron. Mater. 35 (2006) 1621–1627.
[22] H.J. Lin, T.H. Chuanga, J. Alloys Compd. 500 (2010) 167–174.
[23] K.S. Kim, S.H. Huh, K. Suganuma, J. Alloys Compd. 352 (2003) 226–236.
[24] D. Li, C. Liu, P.P. Conway, J. Electron. Mater. 35 (2006) 388–398.
[25] D.Q. Yu, L. Wang, J. Alloys Compd. 458 (2008) 542–547.
[26] Y. Kariya, T. Hosoi, S. Terashima, M. Tanaka, M. Otsuka, J. Electron. Mater. 33 (2004) 321–328.
[27] S.Y. Chang, Y.C. Huang, Y.M. Lin, J. Alloys Compd. 490 (2010) 508–514.
[28] J.H.L. Pang, B.S. Xiong, C.C. Neo, X.R. Zhang, T.H. Low, Proceedings of Electronic Components and Technology Conference, 2003, pp. 673–679.
[29] I. Shohji, T. Yoshida, T. Takahashi, S. Hioki, Mater. Sci. Eng. A 366 (2004) 50–55.
[30] F. Zhu, H. Zhang, R. Guan, S. Liu, J. Alloys Compd. 438 (2007) 100–105.
[31] Y. Xiang, X. Chen, J.J. Vlassak, Proc. Mater. Res. Soc. Symp. 695 (2002), L4.9.1–L4.9.6.
[32] H.D. Merchant, G. Khatibi, B. Weiss, J. Mater. Sci. 39 (2004) 4157–4170.
[33] T. Ventura, C.M. Gourlay, K. Nogita, T. Nishimura, M. Rappaz, A. Dahle, J. Electron. Mater. 37 (2008) 32–39.